Journal of Non-Newtonian Fluid Mechanics 208–209 (2014) 18–26

Contents lists available at ScienceDirect

Journal of Non-Newtonian Fluid Mechanics

journal homepage: http://www.elsevier.com/locate/jnnfm

# Vorticity effects in the non-linear long wavelength convective instability of a viscoelastic fluid layer

I. Pérez-Reyes [a,*], L.A. Dávalos-Orozco [b]

[a] Facultad de Ciencias Químicas, Universidad Autónoma de Chihuahua, Nuevo Campus Universitario, Circuito Universitario S/N, 31125 Chihuahua, Chih., Mexico
[b] Instituto de Investigaciones en Materiales, Departamento de Polímeros, Universidad Nacional Autónoma de México, Ciudad Universitaria, Circuito Exterior S/N, Delegación Coyoacán, 04510 México, D.F., Mexico

ARTICLE INFO

*Article history:*
Received 30 December 2013
Received in revised form 16 March 2014
Accepted 20 March 2014
Available online 30 March 2014

*Keywords:*
Natural convection
Viscoelastic fluid
Pattern selection
Bifurcation

ABSTRACT

The effects of vorticity and poor conductivity boundaries on the non-linear long wavelength instability of an Oldroyd fluid layer heated from below is investigated. It is found a set of two coupled non-linear evolution equations with viscoelastic coefficients. A multiple scales approximation leads to a non-linear Ginzburg–Landau equation which has viscoelastic effects only when the Oldroyd model is corotational and not codeformational. The equation shows an important limitation in the magnitude of the nondimensional relaxation and retardation times. That is, for certain magnitudes of these times, the flow shows no saturation at all. For other magnitudes, the pattern selection is discussed by means of the viscoelastic Ginzburg–Landau equation.



## 1. Introduction

Non-linear convection in viscoelastic fluids have been studied in the past decades for fluid layers confined between two perfectly conducting walls [1–8]. In the present paper new results are reported on the non-linear thermoconvection of a viscoelastic fluid layer between poorly conducting walls. The aim of the present investigation is to clarify the role that inertial effects play in the non-linear instability of a viscoelastic fluid layer. To the authors best knowledge, no research on this important subject has been published in the open literature for Oldroyd viscoelastic fluids. These thermal conditions are relevant in the study of the formation and evolution of convective patterns. Here, it is of interest to make a general analysis of a viscoelastic fluid which includes the upper convected, the lower convected and the corotational Oldroyd fluid models. The non-linear instability of such fluids finds important applications in experimental set-ups, in materials processing and in the food and chemical industries [9–13]. The non-linear stability of a viscoelastic Oldroyd (A, B and corotational) fluid layer between two perfectly conducting walls heated from below has already been reported [3]. Non-linear convection of a second order fluid layer between two insulating walls was investigated previously [14]. More recently, some researchers [4,5,7] have performed calculations on the linear and non-linear convection of binary viscoelastic fluids confined between two perfectly conducting walls. Notice that a review of recent research on viscoelastic natural convection is presented in the paper [15].

All these papers do not include the effects of vorticity which may alter the pattern near the onset of convection through a non-potential term. Therefore, the goal of the present paper is to analyse the role played by vorticity in natural convection of a viscoelastic fluid layer confined between two poorly conducting walls. This problem has already been investigated for Newtonian fluids as can be seen in [16–23]. Here, the goal too is to investigate the pattern formation resulting from the roll-square competition in a square domain and the roll-hexagon competition in a hexagonal domain.

The results of Martínez-Mardones et al. [3] are related to the ideal stress free perfectly conducting walls. In the present investigation the case of rigid poorly thermal conducting walls is addressed. Therefore, the results shown here lead us to understand the behavior of natural convection in an Oldroyd viscoelastic fluid from another standpoint. In their paper Martínez-Mardones et al. [3] studied the problem of stability and pattern selection for the case of oscillatory convection. An interesting finding of that research is that the convective patterns may be modified by small variations in the viscoelastic properties. In their analysis of pattern selection, the patterns only correspond to standing waves. Also, they calculate a Ginzburg–Landau equation for the stationary case, similar in structure to that reported here. However, an important feature of the Ginzburg–Landau equation found in the present

* Corresponding author. Tel.: +52 6141075908.
*E-mail addresses:* ildebrando3@gmail.com (I. Pérez-Reyes), ldavalos@servidor.unam.mx (L.A. Dávalos-Orozco).

http://dx.doi.org/10.1016/j.jnnfm.2014.03.009
0377-0257/

paper is that it shows explicitly the parameters dependence of all the coefficients.

The organization of the paper is as follows. In Section 2 the governing equations and their boundary conditions are outlined as well as a review of the mathematical treatment of the problem. The linear problem is briefly exposed in Section 3. In Section 4 the weakly non-linear analysis is discussed. The patterns stability results are given in Sections 5–7 for rolls, squares and hexagons, respectively. Finally, a discussion is given in Section 8.

## 2. Formulation of the problem

An incompressible viscoelastic fluid layer heated from below, is confined between two infinite horizontal walls perpendicular to gravity which is parallel to the $z^*$-axis. Here, the convective stability of the Oldroyd-A, Oldroyd-B and Oldroyd corotational viscoelastic fluid models is investigated. The first two fluid models are called codeformational, lower convected and upper convected, respectively. The problem assumes that the bounding walls are very poor thermal conductors [24] so that very small but finite Biot numbers take into account the wall to fluid relative thermal conductivities. This situation is different to that of the ideal cases of perfect thermal conducting and thermal insulating walls since a small quantity of heat flux is allowed through the walls. This assumption is used in the thermal boundary conditions. In the case of poorly thermal conducting walls the smallness of the Biot numbers allows to use the shallow water theory approximation [24–26]. The lower and upper walls have temperatures $T_L^*$ and $T_U^*$, respectively, where $T_U^* < T_L^*$. Thus, the governing equations for this problem are the heat equation, the balance of momentum equations and the continuity equation, coupled with the viscoelastic Oldroyd fluid constitutive equations which in dimensional form are

$$\frac{\partial T^*}{\partial t^*} + (\vec{u}^* \cdot \nabla) T^* = \kappa \nabla^2 T^* \tag{1}$$

$$\rho_0 \left( \frac{\partial \vec{u}^*}{\partial t^*} + (\vec{u}^* \cdot \nabla)\vec{u}^* \right) = -\nabla p^* + \nabla \cdot \tau^* + \rho_0 \left[ 1 - \beta (T^* - T_L^*) \right] \vec{g} \tag{2}$$

$$\nabla \cdot \vec{u}^* = 0 \tag{3}$$

$$\left[ 1 + \lambda_1 \left( \frac{\mathrm{D}}{\mathrm{D}t} \right)^* \right] \tau^* = 2\eta_0 \left[ 1 + \lambda_2 \left( \frac{\mathrm{D}}{\mathrm{D}t} \right)^* \right] \mathrm{e}^* \tag{4}$$

The symbol $*$ indicates dimensional variables. In Eqs. (1)–(4), $T^*$ is the fluid temperature, $\vec{u}^* = (u^*, v^*, w^*)$ is the fluid velocity, $p^*$ is the pressure, $\tau^*$ is the stress tensor, $\mathrm{e}^*$ is the shear rate tensor defined below in Eq. (15), $\lambda_1$ is the relaxation time, $\lambda_2$ is the retardation time of the stress, $\rho_0$ is the fluid density, $\eta_0$ is the fluid dynamic viscosity, $\kappa$ is the thermal diffusivity and $t^*$ is the time. $(\mathrm{D}/\mathrm{D}t)^*$ is a non-linear operator standing for lower convective, upper convective and corotational derivatives defined below in this section. In the investigation of the non-linear hydrodynamic stability problem the dependent variables are subjected to finite perturbations. Therefore, the following set of perturbations are considered,

$$\begin{aligned} \vec{u}^* &= \vec{u}_0^* + \vec{u}_1^* \\ T^* &= T_0^* + T_1^* \\ p^* &= p_0^* + p_1^* \end{aligned} \tag{5}$$

where the subscripts 0 and 1 stand for the basic and perturbed states, respectively. In the basic state of the present situation the fluid is at rest, the heat is transferred by conduction and the variables depend on $z^*$ only. In this way $\vec{u}_0^* = 0$ and it can be easily shown that $T_0^* = T_L^* + \Delta T^* z^*/H$. The hydrostatic pressure is $p_0^* = \rho_0 z^* [1 - \beta \Delta T^* z^*/2H] g + p_r^*$ with $p_r^*$ being a reference pressure. The perturbed governing equations are the heat equation, the balance of momentum equations and the continuity equation coupled with the Oldroyd constitutive equations satisfied by the six elements of the shear stress tensor, respectively. These are,

$$\frac{\partial T_1^*}{\partial t^*} + (\vec{u}_1^* \cdot \nabla) T_1^* + w_1^* \frac{dT_0^*}{dz^*} = \kappa \nabla^2 T_1^* \tag{6}$$

$$\rho_0 \left( \frac{\partial \vec{u}_1^*}{\partial t^*} + (\vec{u}_1^* \cdot \nabla)\vec{u}_1^* \right) = -\nabla p_1^* + \nabla \cdot \tau_1^* - \rho_0 \beta g T_1^* \vec{k} \tag{7}$$

$$\nabla \cdot \vec{u}_1^* = 0 \tag{8}$$

$$\left[ 1 + \lambda_1 \left( \frac{\mathrm{D}}{\mathrm{D}t} \right)^* \right] \tau_1^* = 2\eta_0 \left[ 1 + \lambda_2 \left( \frac{\mathrm{D}}{\mathrm{D}t} \right)^* \right] \mathrm{e}_1^* \tag{9}$$

The set of Eqs. (6)–(9) shall be made dimensionless by choosing $\kappa/H, H, H^2/\kappa, \rho\nu\kappa/H^2$ and $\Delta T^*$ as the scalings for velocity, length, time, pressure and temperature, respectively. Thus, in nondimensional form the perturbed governing equations are

$$\frac{\partial T}{\partial t} + (\vec{u} \cdot \nabla) T + w = \nabla^2 T \tag{10}$$

$$Pr^{-1} \left( \frac{\partial \vec{u}}{\partial t} + (\vec{u} \cdot \nabla)\vec{u} \right) = -\nabla p + \nabla \cdot \tau + RT\vec{k} \tag{11}$$

$$\nabla \cdot \vec{u} = 0 \tag{12}$$

$$\left( 1 + F \frac{\mathrm{D}}{\mathrm{D}t} \right) \tau = 2 \left( 1 + FE \frac{\mathrm{D}}{\mathrm{D}t} \right) \mathrm{e} \tag{13}$$

where the superscript $*$ and the subscripts 1 have been dropped out from the perturbed dimensionless variables. $w$ is the vertical component of the velocity $\vec{u}$. The fluid velocity is assumed of the form $\vec{u} = \nabla \times \left( \psi \vec{k} \right) + \nabla \times \nabla \times \left( \chi \vec{k} \right)$, which satisfies Eq. (12). Here, $\vec{k}$ is a unit vertical vector, and $\psi$ and $\chi$ are the toroidal and poloidal potentials. $F = \lambda_1 \kappa / H^2$ and $E = \lambda_2/\lambda_1$ are the nondimensional relaxation time (the Weissenberg number) and the ratio of retardation and relaxation times, whose magnitudes ranges are $0 \leqslant E \leqslant 0.1$ and $0 \leqslant F < \infty$, respectively. Also, $Pr = \nu/\kappa$ is the Prandtl number and $R = g\beta \Delta T^* H^3/\kappa\nu$ is the Rayleigh number. The operator $\mathrm{D}/\mathrm{D}t$ on a tensor $\mathrm{G}$ is defined as

$$\frac{\mathrm{D}\mathrm{G}}{\mathrm{D}t} = \left( \frac{\partial \mathrm{G}}{\partial t} + \vec{u} \cdot \nabla \mathrm{G} \right) + \omega \cdot \mathrm{G} - \mathrm{G} \cdot \omega - a(\mathrm{e} \cdot \mathrm{G} + \mathrm{G} \cdot \mathrm{e}) \tag{14}$$

and it represents the corotational ($a = 0$), the lower convected ($a = -1$) and the upper convected ($a = 1$) time derivatives. Here $\mathrm{e}$ and $\omega$ are the shear rate and the rotation rate tensors defined as the symmetric and antisymmetric parts of the tensor $\nabla \vec{u}$,

$$\nabla \vec{u} = \mathrm{e} + \omega = \frac{1}{2} \left[ \nabla \vec{u} + (\nabla \vec{u})^{Tr} \right] + \frac{1}{2} \left[ \nabla \vec{u} - (\nabla \vec{u})^{Tr} \right] \tag{15}$$

where the superscript $Tr$ stands for the transpose of the tensor. It is important to point out that the definition Eq. (14) only describes the three models time derivatives. Some models allow for the continuous variation of the parameter $a$ in a positive range $0 \leqslant a \leqslant 1$, like in the Johnson–Segalman model [27]. However, in the results given presently, this parameter appears in the expression $1 - a^2$. This only modifies the limiting magnitudes of the Weissenberg number $F$ (except when $a = \pm 1$) where the theory is valid but not the patterns of the convection cells. Therefore, in this paper the values of $a$ are limited to the three cases presented above. The above definition for $\vec{u}$ is now used in the system of Eqs. (10)–(13). Next, the operator curl curl is applied to Eq. (11), splitting the velocity and tensor fields leading to

$$\frac{\partial T}{\partial t} + \left[ \left( \frac{\partial \psi}{\partial y} + \frac{\partial \chi'}{\partial x}, -\frac{\partial \psi}{\partial x} + \frac{\partial \chi'}{\partial y}, -\nabla_\perp^2 \chi \right) \cdot \nabla \right] T - \nabla^2 \chi = \nabla^2 T \tag{16}$$

$$Pr^{-1}\left[-\frac{\partial}{\partial t}\nabla_\perp^2\psi+T_{NL}^1\right]=\left(\frac{\partial^2}{\partial x^2}-\frac{\partial^2}{\partial y^2}\right)\tau_{xy}-\frac{\partial^2}{\partial x\partial y}(\tau_{xx}-\tau_{yy})+\frac{\partial\tau'_{yz}}{\partial x}-\frac{\partial\tau'_{xz}}{\partial y} \quad (17)$$

$$Pr^{-1}\left[\frac{\partial}{\partial t}\left(\nabla_\perp^4\chi+\nabla_\perp^2\chi''\right)+T_{NL}^2\right]=\frac{\partial^2}{\partial x^2}\left(\tau'_{xx}-\tau'_{zz}\right)+\frac{\partial^2}{\partial y^2}\left(\tau'_{yy}-\tau'_{zz}\right)+2\frac{\partial^2\tau'_{xy}}{\partial x\partial y}-\frac{\partial}{\partial x}\nabla_\perp^2\tau_{xz}-\frac{\partial}{\partial y}\nabla_\perp^2\tau_{yz}+\frac{\partial\tau''_{xz}}{\partial x}+\frac{\partial\tau''_{yz}}{\partial y}-R\nabla_\perp^2T \quad (18)$$

where primes mean derivatives with respect to $z$. Here, $\nabla_\perp=(\partial/\partial x,\partial/\partial y)$ is a horizontal vector operator. $T_{NL}^1$ and $T_{NL}^2$ correspond to advective non-linear terms which can be found in Appendix A. Eqs. (16)–(18) are coupled to Eq. (13) which represent the governing equations. The bounding walls are solid so that the boundary conditions for the velocity are translated into those of $\chi$ and $\psi$ as

$$\chi=\chi'=\psi=0 \quad \text{at} \quad z=0,1 \quad (19)$$

The thermal boundary conditions are those for lower and upper poorly thermal conducting walls. These are given in terms of the Biot number as follows,

$$\begin{aligned} T'-B_LT&=0 \quad \text{at} \quad z=0\\ T'+B_UT&=0 \quad \text{at} \quad z=1 \end{aligned} \quad (20)$$

where $B_L$ and $B_U$ are the Biot numbers which account for the heat exchange at the lower and upper walls, respectively.

### 2.1. Evolution equations

As pointed out, here the bounding walls are considered as poorly thermal conductors and in this particular case the Biot numbers $B_L$ and $B_U$ are very small. This means that the ratio of thermal conductivities of the fluid to those of the walls is large and the critical wavenumber for the onset of convection approaches to zero (for more details see Refs. [28,29]). In this case convective motions are slow and take place in a large scale when the heat flux exceeds its critical value. Therefore, the scales in the vertical $z$-axis are smaller than those in the horizontal $x$ and $y$-axes. Thus, based on this discrepancy, a long wavelength approximation [14,18] is performed in order to obtain the non-linear equations to describe the evolution of long-wave planforms. Lets consider $\epsilon\ll 1$ as an expansion parameter which is related to the small quantity of heat flux passing through the walls, physically accounting for the almost insulating characteristic of the walls. A further consequence of this is that $B_{L,U}=O(\epsilon^2)$ or in other words, that $B_{L,U}=\epsilon^2\overline{B}_{L,U}$. Due to the large scale and slowness of the flow, the horizontal coordinates are rescaled by the factor $\epsilon^{1/2}$ [18] and the time by the factor $\epsilon^2$. In the same way, the variables are expanded as follows

$$\chi=\chi_0+\epsilon\chi_1+\epsilon^2\psi_2+\cdots \quad (21)$$
$$\psi=\psi_0+\epsilon\psi_1+\epsilon^2\psi_2+\cdots \quad (22)$$
$$T=\theta_0+\epsilon\theta_1+\epsilon^2\theta_2+\cdots \quad (23)$$
$$R=R_0+\epsilon R_1+\epsilon^2R_2 \quad (24)$$
$$\tau_{xx}=\epsilon\left(\tau_{xx}^{(0)}+\epsilon\tau_{xx}^{(1)}+\epsilon^2\tau_{xx}^{(2)}+\cdots\right) \quad (25)$$
$$\tau_{yy}=\epsilon\left(\tau_{yy}^{(0)}+\epsilon\tau_{yy}^{(1)}+\epsilon^2\tau_{yy}^{(2)}+\cdots\right) \quad (26)$$
$$\tau_{zz}=\epsilon\left(\tau_{zz}^{(0)}+\epsilon\tau_{zz}^{(1)}+\epsilon^2\tau_{zz}^{(2)}+\cdots\right) \quad (27)$$
$$\tau_{xy}=\epsilon\left(\tau_{xy}^{(0)}+\epsilon\tau_{xy}^{(1)}+\epsilon^2\tau_{xy}^{(2)}+\cdots\right) \quad (28)$$
$$\tau_{xz}=\epsilon^{1/2}\left(\tau_{xz}^{(0)}+\epsilon\tau_{xz}^{(1)}+\epsilon^2\tau_{xz}^{(2)}+\cdots\right) \quad (29)$$
$$\tau_{yz}=\epsilon^{1/2}\left(\tau_{yz}^{(0)}+\epsilon\tau_{yz}^{(1)}+\epsilon^2\tau_{yz}^{(2)}+\cdots\right) \quad (30)$$

After a proper rescaling and substitution of the expansion scheme Eqs. (21)–(30) into Eqs. (13)–(20), a system of differential equations is obtained at each different order of $\epsilon$, subjected to their corresponding boundary conditions at the same order. The resulting systems of differential equations are large. For the sake of clarity they are listed in Appendix B. Some analytical solutions are given below. Thus, at $O(1)$, Eq. (B.3) is subjected to boundary conditions Eq. (B.10) with the solution

$$\theta_0=\Phi(x,y,\bar{t}) \quad (31)$$

Next, the velocity component $\chi_0$ can be obtained as follows: Eqs. (B.6) and (B.8) are operated with $\partial''/\partial x$ and $\partial''/\partial y$ and substituted into Eq. (B.1). Then, $\chi_0$ can be calculated subjected to boundary conditions Eq. (B.11) to give,

$$\chi_0=\frac{R_0}{24}z^2(z-1)^2\Phi(x,y,\bar{t}) \quad (32)$$

On the other hand, for the other potential the solution is $\psi_0=0$. A similar process as that followed for $\chi_0$ was used in combination with Eq. (B.2) and boundary conditions Eq. (B.12). The same procedure used above was repeated at $O(\epsilon)$ to calculate $\theta_1,\chi_1$ and $\psi_1$, whose expressions are very large and are not presented here. At $O(\epsilon)$ a solvability condition obtained from the temperature Eq. (B.15) should be satisfied. Then, after integration of Eq. (B.15) with respect to $z$ across the fluid layer, the result is $R_0=720$.

Later in the solution process [18] at $O(\epsilon^2)$ a second solvability condition should be satisfied too. This one is calculated from Eqs (B.25) and boundary conditions Eqs. (B.26) and (B.27). As before, Eq. (B.25) is integrated across the fluid layer and the Biot numbers are then included by using Eqs. (B.26) and (B.27). Therefore, the following set of evolution equations are found for the three Oldroyd fluid models,

$$\begin{aligned}\frac{\partial\Phi}{\partial t}=&-(B_U+B_L)\Phi+\left(1-\frac{R}{720}\right)\nabla_\perp^2\Phi-\frac{17}{462}\nabla_\perp^4\Phi\\&+\frac{10}{7}\left[1-1080F^2(1-E)(1-a^2)\right]\\&\times\nabla_\perp[(\nabla_\perp\Phi)(\nabla_\perp\Phi\cdot\nabla_\perp\Phi)]\\&+\left[\frac{15}{7}Pr^{-1}-F(1-E)\left(\frac{540}{7}+60a\right)\right]\times\nabla_\perp\Phi\wedge\nabla_\perp\Psi\end{aligned} \quad (33)$$

$$\nabla_\perp^2\Psi=\nabla_\perp\Phi\wedge\nabla_\perp\left(\nabla_\perp^2\Phi\right) \quad (34)$$

The vector product $\wedge$ is defined by $\nabla_\perp f(x,y)\wedge\nabla_\perp g(x,y)=(\partial f/\partial y)(\partial g/\partial x)-(\partial f/\partial x)(\partial g/\partial y)$. In Eqs. (33) and (34) the function $\Psi$ represents effects of vorticity since the last non-linear terms in Eq. (33) are a direct contribution of the solution $\psi_1$, obtained at $O(\epsilon)$. In the literature these terms are referred to as non-potential terms accounting for inertial effects and for a mean drift flow. Notice that Eq. (33) reduces to that for the Newtonian fluid [18] when the viscoelastic effects are zero ($F=0$). Moreover, note that the influence of viscoelasticity only appears in the non-linear terms. This means that, under the present approximation, the Rayleigh number obtained from the linear theory does not depend on $E$ and the Weissenberg number $F$. This is due to the small time variation of the flow when the Biot numbers are small. Under these conditions, the convective cells are extremely large and the flow is nearly parallel in the center of the cells. It is clear in the evolution Eq. (33) that when $a=\pm1$ the influence of viscoelasticity only appears in the last term coupled with vorticity. Then, for the three fluid models, the condition $15/(7Pr)-F(1-E)(540/7+60a)\neq0$ must be satisfied to have the vorticity effects acting on viscoelastic convection. If this coefficient is assumed positive, its magnitude would be larger for the lower convected fluid ($a=-1$), next for the corotational fluid ($a=0$) and finally, the smallest magnitude

would correspond to the upper convected fluid ($a = 1$). Therefore, the interaction with vorticity decreases, in the same order, for each Oldroyd fluid model. On the other hand, for the corotational Oldroyd fluid ($a = 0$), the coefficient of the first non-linear term of Eq. (33), that is $1 - 1080F^2(1 - E)$ (independent of $Pr$), will play an important role on the stability, as will be shown presently. This coefficient can become zero and even change sign depending on the magnitudes of the Weissenberg number $F$ and $E$. For example, if $E = 0.1$ that coefficient becomes zero at the small value of $F = 0.032$. The changes of sign will be interpreted below from the point of view of nonlinear stability.

## 3. The linear problem

We consider the linear stability of natural convection between poorly conducting horizontal boundaries with respect to disturbances which are proportional to $\exp\left[i(k_x x + k_y y) + \sigma t\right]$, where $k_x$ and $k_y$ are the $x$ and $y$-components of the wavenumber vector with magnitude $k = \sqrt{k_x^2 + k_y^2}$. $\sigma$ is a complex parameter whose real $\sigma_R$ and imaginary $\sigma_I$ parts are the growth rate and the frequency of oscillation, respectively. It has been found that, under the present approximation, the frequency of oscillation is zero and that consequently the linear behavior of the fluid is Newtonian. Thus, Eqs. (35) and (36) agree with the results reported by Pismen [18] after taking into account that $B_U, B_L = \pm\epsilon/2$ in that paper. The critical Rayleigh number and wavenumber of stationary convection are:

$$R_c = 720\left[\left(\frac{34(B_U + B_L)}{231}\right)^{1/2} + 1\right] \tag{35}$$

$$k_c = \left(\frac{462(B_U + B_L)}{17}\right)^{1/4} \tag{36}$$

where $B_U$ and $B_L$ are the Biot numbers at the lower and upper walls. Notice that Eqs. (35) and (36) correspond to the classical result of insulating walls when $B_U, B_L = 0$. That is, $R_c = 720$ and $k_c = 0$. Therefore, Eqs. (35) and (36) show the corrections when the approximation agrees with small but finite Biot numbers. In Fig. 1 two samples of convection cells at criticality are plotted for two different Biot numbers assuming that the upper and lower walls have the same thermal properties. Notice the large contrast between the scales of vertical and horizontal axes. Moreover, note that the number of convection cells is larger in Fig. 1a in comparison with Fig. 1b, as expected for long wavelength convection.

## 4. Weakly non-linear theory

Here, we investigate the weakly non-linear behavior of the solutions to Eqs. (33) and (34) for the three fluid models mentioned above. We consider that $R$ is close to $R_c$ so that $R = R_c + \delta^2\overline{R}$, where $R_c$ is defined in Eq. (35) and $\delta$ is a small parameter related to the separation from criticality $(R - R_c)/\overline{R}$. The procedure followed here in the weakly non-linear analysis has been used before by other authors [19,30–32]. It is considered that the functions in Eqs. (33) and (34) have an asymptotic behavior. The functions are expanded in power series as $\Phi = \delta\Phi_1 + \delta^2\Phi_2 + \cdots$ and $\Psi = \delta\Psi_1 + \delta^2\Psi_2 + \cdots$ and they are substituted into Eqs. (33) and (34). Then, for slow spatial and temporal modulations the following expansions for $(x, y, t)$ are used

$$\begin{aligned}
\frac{\partial}{\partial x} &\to \frac{\partial}{\partial x} + \delta\frac{\partial}{\partial \mathbf{X}} + \delta^2\frac{\partial}{\partial \mathbf{X}_2}\\
\frac{\partial}{\partial y} &\to \frac{\partial}{\partial y} + \delta\frac{\partial}{\partial \mathbf{Y}} + \delta^2\frac{\partial}{\partial \mathbf{Y}_2}\\
\frac{\partial}{\partial t} &\to \delta^2\frac{\partial}{\partial \bar{t}} + \delta^3\frac{\partial}{\partial \bar{t}_2}
\end{aligned} \tag{37}$$

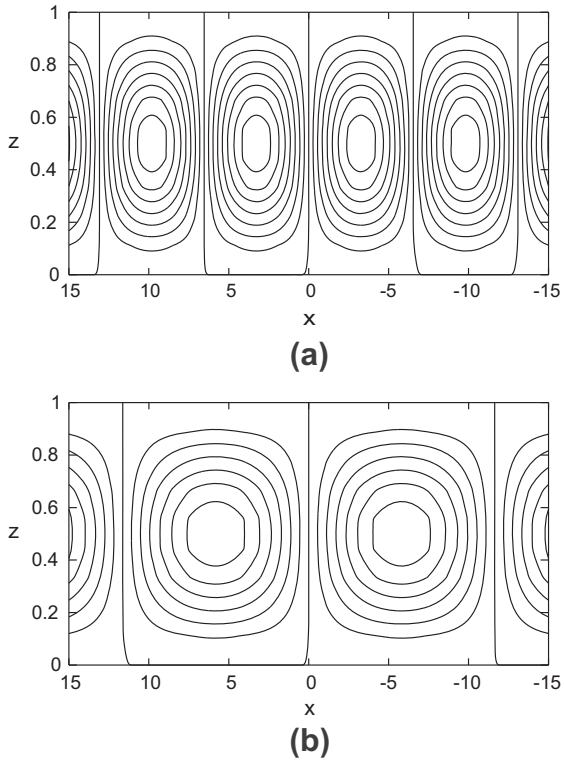


**Fig. 1.** Convection cells. (a) For Biot numbers $B_U = B_L = 0.001$ the critical wavenumber and Rayleigh number are $k_c = 0.48$ and $R_c = 732.35$, respectively. (b) For Biot numbers $B_U = B_L = 0.0001$ the critical wavenumber and Rayleigh number are $k_c = 0.27$ and $R_c = 723.91$, respectively.

where $\mathbf{X}, \mathbf{X}_2, \mathbf{Y}, \mathbf{Y}_2, \bar{t}, \bar{t}_2$ are slow spatial and temporal variables. The procedure follows the method of Newell–Whitehead–Segel [33,34]. It is well known that the convection flow is very slow when the Biot numbers are small. Therefore, it is assumed that the time variation of the flow is also small and the expansion of the time derivatives start with $\delta^2$.

## 5. Steady roll patterns

The solution at $O(\delta)$ is assumed to be of the form

$$\Phi_1 = A(\mathbf{X}, \mathbf{Y}, \bar{t})\exp(ik_c x) + c.c. \tag{38}$$

where $c.c.$ stands for complex conjugate. At $O(\delta^2)$ it is found that $\Phi_2 = 0$. At $O(\delta^3)$ the evolution equation of $A$ is found as the corresponding solvability condition. Therefore, $A$ satisfies

$$\begin{aligned}
\frac{\partial A}{\partial \bar{t}} = {} & \frac{\overline{R}}{720}k_c^2 A + \frac{34}{231}k_c^2\left(\frac{\partial}{\partial \mathbf{X}} - \frac{i}{2k_c}\frac{\partial^2}{\partial \mathbf{Y}^2}\right)^2 A\\
& - \frac{30}{7}\left[1 - 1080F^2(1 - E)(1 - a^2)\right]k_c^4 A|A|^2
\end{aligned} \tag{39}$$

By using suitable scalings on $A, \mathbf{X}$ and $\mathbf{Y}$ we arrive at the canonical form for the amplitude equation

$$\frac{\partial \overline{A}}{\partial \bar{t}} = r\overline{A} + \left(\frac{\partial}{\partial \overline{\mathbf{X}}} - i\frac{\partial^2}{\partial \overline{\mathbf{Y}}^2}\right)^2 \overline{A} - \overline{A}|\overline{A}|^2 \tag{40}$$

where $r = \overline{R}k_c^2/720$. Eq. (40) is the same as that derived first by Newell–Segel–Whitehead [33,34] which corresponds to convective rolls oriented on the $y$ axis. Care must be taken here, because in the viscoelastic case the coefficient $1 - 1080F^2(1 - E)(1 - a^2)$ can be zero and it is not possible to obtain this canonical form. In case that

this coefficient is negative the equation differs from that of Newell–Whitehead–Segel [33,34]. Notice that there is a supercritical bifurcation when the coefficient $1-1080F^2(1-E)(1-a^2)>0$ in Eq. (39). When $a=\pm1$ the condition is readily satisfied and the equation is the same as the Newtonian one. For the corotational Oldroyd fluid, with $a=0$, the condition for supercritical bifurcation changes into $F^2<1/1080(1-E)$. Here, the magnitude of $E$ cannot be one. In fact, its value must be $E\leqslant 0.1$. As explained above, the largest possible value of the Weissenberg number $F$ is smaller than 0.032 if $E=0.1$. Conversely, if $1-1080F^2(1-E)<0$ the bifurcation is subcritical and no saturation occurs. Then, the amplitude $|\overline{A}|$ increases with time without limit. There is no saturation too when the equality holds because the non-linear term is zero. Similar findings have been reported [3] for the case of convection in a viscoelastic fluid confined between two perfectly conducting walls.

In this way, under the present small wavenumber approximation and close to the point of criticality, the amplitude equation for convective rolls has a structure similar to that of the Newtonian fluid. The difference appears in the coefficient of the non-linear term which only depends on viscoelasticity when the Oldroyd fluid is corotational. This certainly will be reflected in the non-linear growth rate of rolls. In view of the canonical form of Eq. (40) the stability analysis for rolls is the same as that already reported [35–38]. This result was unexpected due to the presence of the Biot number which sets the system a little far from the ideal situation of insulating walls, already studied for example, in the convection of a second order fluid [14].

## 6. Roll and square patterns in a square lattice

Rolls and squares may arise in a square lattice and compete between each other. Thus, the following solution at $O(\delta)$ for two sets of rolls at right angles is assumed

$$\Phi_1=A(\mathbf{X},\mathbf{Y},\bar{t})\exp(ik_cx)+B(\mathbf{X},\mathbf{Y},\bar{t})\exp(ik_cy)+c.c. \tag{41}$$

The process is the same as before and the following amplitude equations for the two sets of rolls are obtained

$$\frac{\partial A}{\partial\bar{t}}=\frac{\overline{R}}{720}k_c^2A+\frac{34}{231}k_c^2\frac{\partial^2A}{\partial\mathbf{X}^2}-\frac{30}{7}\left[1-1080F^2(1-E)(1-a^2)\right]\times k_c^4A\left(|A|^2+\frac{2}{3}|B|^2\right) \tag{42}$$

$$\frac{\partial B}{\partial\bar{t}}=\frac{\overline{R}}{720}k_c^2B+\frac{34}{231}k_c^2\frac{\partial^2B}{\partial\mathbf{Y}^2}-\frac{30}{7}\left[1-1080F^2(1-E)(1-a^2)\right]\times k_c^4B\left(|B|^2+\frac{2}{3}|A|^2\right) \tag{43}$$

The amplitude Eqs. (42) and (43) show explicitly the presence of the viscoelastic effects contributed by the three models mentioned above. Notice that the viscoelastic parameters can be factorized in the crossed cubic terms which establish the interaction between $A$ and $B$ rolls. In this case, roll and square patterns are able to appear and they have the following steady solutions.

- $A$ rolls:

$$A_0=\sqrt{\frac{\frac{\overline{R}}{720}k_c^2}{\frac{30}{7}\left[1-1080F^2(1-E)(1-a^2)\right]k_c^4}} \tag{44}$$
$$B_0=0$$

- squares

$$A_0=B_0=\sqrt{\frac{\frac{\overline{R}}{720}k_c^2}{\frac{50}{7}\left[1-1080F^2(1-E)(1-a^2)\right]k_c^4}} \tag{45}$$

where no spatial modulation was taken into account. The bifurcation theory on a square lattice [35,37] gives interesting results on the stability of rolls and squares. The result is that the rolls are unstable, while the square patterns always are stable. This is due to the factor 2/3 appearing in the cross terms of the amplitude Eqs. (42) and (43). This also means that the interaction between the two rolls is not influenced by viscoelastic effects. The result is obtained applying a small perturbation to the square solutions. It is found that for stability, the coefficient of the $A$ cubic term in Eq. (42) should be greater than that of the quadratic crossed term $AB$. The same is valid for Eq. (43). This agrees with previous results [35–38]. In those papers it is shown that when the magnitude of the coefficient of the quadratic crossed term $AB$ is less that 1, the squares are preferred over rolls close to the onset. Here, this term is zero and does not appear. Therefore, the condition for stable squares reduces to

$$\frac{\overline{R}}{720}k_c^2>0 \tag{46}$$

The bifurcation diagram for this case is shown in Fig. 2 and it summarizes the results discussed previously. As in the preceding section for rolls, the viscoelastic properties of the fluid only survive in Eqs. (42) and (43) when $a=0$ for the Oldroyd corotational fluid. Viscoelasticity has influence on the size of the patterns but not on the stability, except when the coefficient of the cubic terms is zero or negative.

## 7. Roll and hexagon patterns in a hexagonal lattice

Hexagonal cells and rolls may also exist near the onset of convection. Therefore, a hexagonal lattice is considered to investigate the stability of these patterns. The form of the solution at $O(\delta)$ for the set of three rolls, at an angle of 60° to each other, is the following

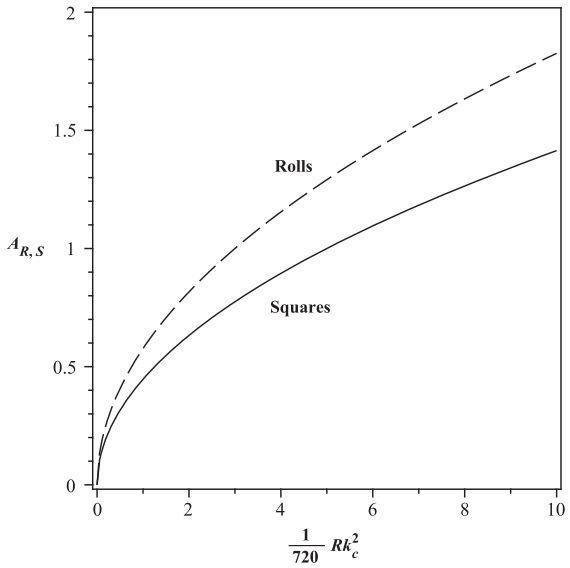


**Fig. 2.** Bifurcation diagram of rolls and squares in a square domain. The dashed line means instability of the labeled structure while the solid line indicates stable patterns, respectively. The subscript $R,S$ was added to the amplitude steady solution to point out that it has been divided by $(10/7)\left[1-1080F^2(1-E)(1-a^2)\right]k_c^4$.

$$\Phi_1 = A(\mathbf{X},\mathbf{Y},\bar{t})\exp(ik_c x) + B(\mathbf{X},\mathbf{Y},\bar{t})\exp\left[\frac{ik_c}{2}\left(-x+\sqrt{3}y\right)\right] + C(\mathbf{X},\mathbf{Y},\bar{t})\exp\left[-\frac{ik_c}{2}\left(x+\sqrt{3}y\right)\right] + c.c. \quad (47)$$

The same process is followed as before to obtain the amplitude equations

$$\frac{\partial A}{\partial \bar{t}} = \frac{\bar{R}}{720}k_c^2 A + \frac{34}{231}k_c^2\frac{\partial^2 A}{\partial \mathbf{X}^2} - \frac{30}{7}\left[1-1080F^2(1-E)(1-a^2)\right] \times k_c^4 A\left(|A|^2+|B|^2+|C|^2\right) \quad (48)$$

$$\frac{\partial B}{\partial \bar{t}} = \frac{\bar{R}}{720}k_c^2 B + \frac{34}{231}k_c^2\frac{\partial^2 B}{\partial \xi^2} - \frac{30}{7}\left[1-1080F^2(1-E)(1-a^2)\right] \times k_c^4 B\left(|A|^2+|B|^2+|C|^2\right) \quad (49)$$

$$\frac{\partial C}{\partial \bar{t}} = \frac{\bar{R}}{720}k_c^2 C + \frac{34}{231}k_c^2\frac{\partial^2 C}{\partial \eta^2} - \frac{30}{7}\left[1-1080F^2(1-E)(1-a^2)\right] \times k_c^4 C\left(|A|^2+|B|^2+|C|^2\right) \quad (50)$$

where $\xi = \left(-\mathbf{X}+\sqrt{3}\mathbf{Y}\right)/2$ and $\eta = \left(-\mathbf{X}-\sqrt{3}\mathbf{Y}\right)/2$. Observe that as in the square lattice case, the viscoelastic parameters only appear as a non-linear effect and they can be factorized in front of the cubic terms. It is important to notice that the non-linear interactions in all the cubic terms have the same weight for the set of three rolls. This characteristic of Eqs. (48)–(50) is a result of the symmetry imposed by the rigid–rigid boundary conditions considered here. For the asymmetric rigid-free boundary conditions the coefficients are different in the coupling of the non-linear terms [30,35–38]. Similar findings to those reported here have been published in [30].

When modulations are neglected, Eqs. (48)–(50) have the following steady equilibrium solutions for rolls and hexagons.

- A rolls

$$A_0 = \sqrt{\frac{\frac{\bar{R}}{720}k_c^2}{\frac{30}{7}\left[1-1080F^2(1-E)(1-a^2)\right]k_c^4}} \quad (51)$$
$$B_0 = C_0 = 0$$

- hexagons

$$A_0 = B_0 = C_0 = \sqrt{\frac{\frac{\bar{R}}{720}k_c^2}{\frac{90}{7}\left[1-1080F^2(1-E)(1-a^2)\right]k_c^4}} \quad (52)$$

Notice that the roll solution Eq. (51) is the same as Eq. (44) found in the square lattice analysis. Therefore, roll patterns are possible in both the square and the hexagonal lattices. Thus, it is reasonable to obtain the same solution in both cases. Again, the viscoelastic properties only appear for the Oldroyd corotational fluid ($a = 0$) and these influence the size of the patterns.

Considering that the system of Eqs. (48)–(50) can be rewritten in a canonical form as in the case of rolls, it follows that the coefficient of the cubic terms has no influence on the pattern stability, except when it is zero or negative. In other words, the pattern selection problem in a hexagonal lattice is similar to that found in the stability of a Newtonian fluid layer. A complete analysis on the stability of hexagons and rolls in a hexagonal lattice is provided by Fujimura and Yamada [39]. Thus, the solution of the present problem shall be undertaken with the help of their results. It is found that, in the absence of quadratic coupling terms, only rolls are stable in a hexagonal lattice near criticality. However, hexagons and rolls are simultaneously stable for magnitudes of $\bar{R}k_c^2/720$ a little far from criticality.

Two notable features of the amplitude Eqs. (48)–(50) are therefore the absence of a quadratic coupling term and the identical coefficients in the cubic terms. It is pointed out here that the structure of that set of amplitude equations in this case does not allow the applicability of the method used before [35]. This is mainly due to the symmetry of the problem and to the Boussinesq approximations.

## 8. Discussion

The main result of this paper is the calculation of the evolution Eqs. (33) and (34) which include inertial effects through a coupling non-linear term for the corotational, upper and lower convected Oldroyd fluids. This term makes the evolution equations more general than those reported before [18,19,24]. As found for the Newtonian case [18], the so called mean drift flow is very weak near the instability threshold, and thus it has no influence in the convective pattern selection. It is important to note that, under the present approximation, the linear stability is not influenced by viscoelasticity and that the onset of convection is stationary. A similar result has been found for the linear thermoconvective stability of a viscoelastic Maxwell fluid layer heated from below [28]. There, it is shown that a codimension-two point exists separating stationary and oscillatory convection which depends on the magnitude of the Prandtl and Biot numbers. In the present paper, it is found that the bifurcation is supercritical for any of the three viscoelastic fluids considered if $1-1080F^2(1-E)>0$ which is the coefficient of the cubical term of Eq. (39). Subcriticality occurs when it is negative. It is clear that the stability of the Newtonian fluid always is supercritical and the solution always attains saturation. This saturation condition limits the magnitude of the Weissenberg number $F$ and $E$ of the corotational Oldroyd fluid. The problem is that the magnitudes of the Weissenberg number are restricted to a very small range of values. From the multiple scales approximation, it is clear that the inertial effects of vorticity do not appear in the Ginzburg–Landau equations. The scaling assumed for the variables in the derivation of the amplitude equation shows that one of the roles of viscoelasticity is to modify the amplitude and size of the convection patterns. Moreover, due to the rigid–rigid boundary conditions assumed from the beginning, viscoelasticity will also change the shear stresses at the walls. The pattern selection studied from the geometrical point of view in a squared domain shows that squares are stable and rolls unstable. As before, viscoelasticity is only important for the corotational fluid. For the situation in a hexagonal domain, the stability of rolls and hexagons is investigated using the results of Fujimura and Yamada [39]. It is found that (see [39]), in the absence of quadratic coupling terms, only rolls are stable near criticality. A further increase of $\bar{R}k_c^2/720$ leads to the simultaneous stability of rolls and hexagons in a hexagonal lattice. Based on the results of Ref. [39] it is important to point out that the set of amplitude equations studied here may be considered as an $O(1)$ approximation to the small quadratic and cubic coupling terms in a more general set of amplitude equations [35].

## Acknowledgments

The authors would like to thank, Joaquín Morales, Cain González, Raúl Reyes, Alberto López, Ma. Teresa Vázquez and Oralia Jiménez for technical support. I. Pérez Reyes would like to thank the Programa de Mejoramiento del Profesorado (PROMEP).

## Appendix A. Convective non-linear terms

This appendix gives the large non-linear terms $T^1_{NL}$ and $T^2_{NL}$ appearing in Eqs. (17) and (18). They are:

$$\begin{aligned} T^1_{NL} = &-\nabla_\perp\left(\nabla^2_\perp\chi\right) \wedge \nabla_\perp\chi'' + \nabla_\perp\left(\nabla^2_\perp\chi\right)\cdot(\nabla_\perp\psi') \\ &- \nabla_\perp\left(\nabla^2_\perp\psi\right)\cdot(\nabla_\perp\chi') + \nabla_\perp\left(\nabla^2_\perp\psi\right) \wedge \nabla_\perp\psi \\ &+ \left(\nabla^2_\perp\psi'\right)\left(\nabla^2_\perp\chi\right) - \left(\nabla^2_\perp\psi\right)\left(\nabla^2_\perp\chi'\right) \end{aligned} \tag{A.1}$$

$$\begin{aligned} T^2_{NL} = &\left(\frac{\partial^2\chi''}{\partial x^2} - \frac{\partial^2\chi''}{\partial y^2} + \frac{\partial^4\chi}{\partial x^4} - \frac{\partial^4\chi}{\partial y^4} + 2\frac{\partial^2\psi'}{\partial x\partial y}\right)\left(\frac{\partial^2\chi'}{\partial x^2} - \frac{\partial^2\chi'}{\partial y^2} + 2\frac{\partial^2\psi}{\partial x\partial y}\right) \\ &- \left(\nabla^4_\perp\chi' + \nabla^2_\perp\chi'''\right)\nabla^2_\perp\chi - \nabla_\perp\left(\nabla^2_\perp\psi - \psi''\right) \\ &\wedge \nabla_\perp\left(\nabla^2_\perp\chi\right) + \nabla_\perp\left(\nabla^4_\perp\chi + \nabla^2_\perp\chi''\right) \wedge \nabla_\perp\psi \\ &- 2\frac{\partial^2}{\partial x\partial y}\nabla^2\chi\left(\frac{\partial^2\psi}{\partial x^2} - \frac{\partial^2\psi}{\partial y^2}\right) - 2\left(\frac{\partial^2\psi'}{\partial y^2}\frac{\partial^2\psi}{\partial x^2} + \frac{\partial^2\psi'}{\partial x^2}\frac{\partial^2\psi}{\partial y^2}\right) \\ &+ 2\left(2\frac{\partial^2}{\partial x\partial y}\nabla^2\chi + \frac{\partial^2\psi'}{\partial y^2} - \frac{\partial^2\psi'}{\partial x^2}\right)\frac{\partial^2\chi'}{\partial x\partial y} \\ &+ \nabla_\perp\left(\nabla^4_\perp\chi + \nabla^2_\perp\chi''\right)\cdot(\nabla_\perp\chi') - \nabla_\perp\left(\nabla^2\chi'\right)\cdot\nabla_\perp\left(\nabla^2_\perp\chi\right) \end{aligned} \tag{A.2}$$

## Appendix B. Systems of equations

This Appendix presents the systems of equations used to compute the final evolution equations given in Section 2.1. The following expressions correspond to $O(1)$. From Eq. (18):

$$0 = \frac{\partial\tau^{(0)''}_{xz}}{\partial x} + \frac{\partial\tau^{(0)''}_{yz}}{\partial y} - R_0\nabla^2_\perp\theta_0 \tag{B.1}$$

From Eq. (17):

$$0 = \frac{\partial\tau^{(0)'}_{yz}}{\partial x} - \frac{\partial\tau^{(0)'}_{xz}}{\partial y} \tag{B.2}$$

From Eq. (13) for the temperature:

$$0 = \frac{\partial^2\theta_0}{\partial z^2} \tag{B.3}$$

The expressions for $\tau^{(0)}_{xx}, \tau^{(0)}_{xy}, \tau^{(0)}_{xz}, \tau^{(0)}_{yy}, \tau^{(0)}_{yz}$ and $\tau^{(0)}_{zz}$ are,

$$\begin{aligned} 0 = &\tau^{(0)}_{xx} + (1+a)F\left(\frac{\partial\psi'_0}{\partial y} + \frac{\partial\chi''_0}{\partial x}\right)\left[E\left(\frac{\partial\psi'_0}{\partial y} + \frac{\partial\chi''_0}{\partial x}\right) - \tau^{(0)}_{xz}\right] \\ &- 2\left(\frac{\partial^2\psi_0}{\partial x\partial y} + \frac{\partial^2\chi_0}{\partial x^2}\right) \end{aligned} \tag{B.4}$$

$$\begin{aligned} 0 = &\tau^{(0)}_{xy} + \frac{F}{2}(1+a)\left[\tau^{(0)}_{xz}\left(\frac{\partial\psi'_0}{\partial x} - \frac{\partial\chi''_0}{\partial y}\right)\right. \\ &\left. - \tau^{(0)}_{yz}\left(\frac{\partial\psi'_0}{\partial y} + \frac{\partial\chi''_0}{\partial x}\right)\right]FE(1+a)\left(\frac{\partial\psi'_0}{\partial x} - \frac{\partial\chi''_0}{\partial y}\right)\left(\frac{\partial\psi'_0}{\partial y} + \frac{\partial\chi''_0}{\partial x}\right) \\ &- \frac{\partial^2\psi_0}{\partial y^2} + \frac{\partial^2\psi_0}{\partial x^2} - 2\frac{\partial^2\chi_0}{\partial x\partial y} \end{aligned} \tag{B.5}$$

$$0 = \tau^{(0)}_{xz} - \frac{\partial\psi'_0}{\partial y} - \frac{\partial\chi''_0}{\partial x} \tag{B.6}$$

$$\begin{aligned} 0 = &\tau^{(0)}_{yy} + F(1+a)\left(\frac{\partial\psi'_0}{\partial x} - \frac{\partial\chi''_0}{\partial y}\right)\left[E\left(\frac{\partial\psi'_0}{\partial x} - \frac{\partial\chi''_0}{\partial y}\right) + \tau^{(0)}_{yz}\right] \\ &+ 2\frac{\partial^2\psi_0}{\partial x\partial y} - 2\frac{\partial^1\chi'_0}{\partial y^2} \end{aligned} \tag{B.7}$$

$$0 = \tau^{(0)}_{yz} + \frac{\partial\psi'_0}{\partial x} - \frac{\partial\chi''_0}{\partial y} \tag{B.8}$$

$$\begin{aligned} 0 = &\tau^{(0)}_{zz} - FE(1-a)\left[\left(\frac{\partial\psi'_0}{\partial x} - \frac{\partial\chi''_0}{\partial y}\right)^2 + \left(\frac{\partial\psi'_0}{\partial y} + \frac{\partial\chi''_0}{\partial x}\right)^2\right] - F(1 \\ &- a)\left[\tau^{(0)}_{yz}\left(\frac{\partial\psi'_0}{\partial x} - \frac{\partial\chi''_0}{\partial y}\right) - \tau^{(0)}_{xz}\left(\frac{\partial\psi'_0}{\partial y} + \frac{\partial\chi''_0}{\partial x}\right)\right] + 2\nabla^2_\perp\chi'_0 \end{aligned} \tag{B.9}$$

At this order the proper boundary conditions are,

$$\frac{\partial\theta_0}{\partial z} = 0 \quad \text{at} \quad z = 0, 1 \tag{B.10}$$

$$\frac{\partial\chi_0}{\partial z} = \chi_0 = 0 \quad \text{at} \quad z = 0, 1 \tag{B.11}$$

$$\psi_0 = 0 \quad \text{at} \quad z = 0, 1 \tag{B.12}$$

From Eqs. (B.3), (B.6) and (B.8) together with the boundary condition Eq. (B.12), it is found that $\psi_0 = 0$. With this the equations at $O(\epsilon)$ are simplified. Further simplifications can also be made with the solution to Eq. (B.3) subjected to boundary condition Eq. (B.10). This leads to the result that $\theta_0(x,y,z,t) = \Phi(x,y,t)$, is independent of $z$. Then, from Eq. (18):

$$\begin{aligned} &\frac{1}{Pr}\left[\left(\frac{\partial\chi''_0}{\partial x^2} - \frac{\partial\chi''_0}{\partial y^2}\right)\left(\frac{\partial\chi'_0}{\partial x^2} - \frac{\partial\chi'_0}{\partial y^2}\right) - \left(\nabla^2_\perp\chi'''_0\right)\left(\nabla^2_\perp\chi_0\right)\right. \\ &\left. -(\nabla_\perp\chi'''_0)\cdot\nabla_\perp\left(\nabla^2_\perp\chi_0\right) + 4\frac{\partial^2\chi'_0}{\partial x\partial y}\frac{\partial^2\chi''_0}{\partial x\partial y} + \nabla_\perp\left(\nabla^2_\perp\chi''_0\right)\cdot(\nabla_\perp\chi'_0)\right] \\ &= -R_0\nabla^2_\perp\theta_1 - R_1\nabla^2_\perp\theta_0 - \nabla^2_\perp\tau^{(0)'}_{zz} - \frac{\partial}{\partial y}\left(\nabla^2_\perp\tau^{(0)}_{yz}\right) - \frac{\partial}{\partial x}\left(\nabla^2_\perp\tau^{(0)}_{xz}\right) \\ &+ \frac{\partial^2}{\partial x^2}\tau^{(0)'}_{xx} + 2\frac{\partial^2}{\partial x\partial y}\tau^{(0)'}_{xy} + \frac{\partial}{\partial y}\tau^{(1)''}_{yz} + \frac{\partial^2}{\partial y^2}\tau^{(0)'}_{yy} \end{aligned} \tag{B.13}$$

From Eq. (17):

$$\begin{aligned} \frac{1}{Pr}\left[-\nabla_\perp\left(\nabla^2_\perp\chi_0\right) \wedge \nabla_\perp\chi''_0\right] = &-\nabla^2_\perp\tau^{(0)}_{xy} + \frac{\partial^2}{\partial x\partial y}\left[\tau^{(0)}_{yy} - \tau^{(0)}_{xx}\right] \\ &+ \frac{\partial}{\partial x}\tau^{(1)'}_{yz} - \frac{\partial}{\partial y}\tau^{(1)'}_{xz} \end{aligned} \tag{B.14}$$

From the temperature Eq. (13):

$$\frac{\partial\chi'_0}{\partial x}\frac{\partial\theta_0}{\partial x} + \frac{\partial\chi'_0}{\partial y}\frac{\partial\theta_0}{\partial y} = -\nabla^2_\perp\chi_0 + \nabla^2_\perp\theta_0 + \frac{\partial^2\theta_1}{\partial z^2} \tag{B.15}$$

Next, the expressions for $\tau^{(1)}_{xx}, \tau^{(1)}_{xy}, \tau^{(1)}_{xz}, \tau^{(1)}_{yy}, \tau^{(1)}_{yz}$ and $\tau^{(1)}_{zz}$ are,

$$\begin{aligned} 0 = &F\left[-2a\left(\tau^{(0)}_{xx}\frac{\partial^2\chi'_0}{\partial x^2} + \tau^{(0)}_{xy}\frac{\partial^2\chi'_0}{\partial x\partial y}\right) - (1+a)\left(\tau^{(0)}_{xz}\left(\frac{\partial\chi''_1}{\partial x} + \frac{\partial\psi'_1}{\partial y}\right)\right.\right. \\ &\left.\left. + \tau^{(1)}_{xz}\frac{\partial\chi''_0}{\partial x}\right) - (1-a)\tau^{(0)}_{xz}\frac{\partial\nabla^2_\perp\chi_0}{\partial x} - \tau^{(0)'}_{xx}\nabla^2_\perp\chi_0 + \frac{\partial\chi'_0}{\partial y}\frac{\partial\tau^{(0)}_{xx}}{\partial y} + \frac{\partial\chi'_0}{\partial x}\frac{\partial\tau^{(0)}_{xx}}{\partial x}\right] \\ &- 2FE\left[-2a\left(\left(\frac{\partial^2\chi'_0}{\partial x^2}\right)^2 + \left(\frac{\partial^2\chi'_0}{\partial x\partial y}\right)^2\right) - \frac{1+a}{2}\left(\frac{\partial\chi''_0}{\partial x} + \frac{\partial\chi'_0}{\partial x}\right)\right. \\ &\left(\frac{\partial\psi'_1}{\partial y} + \frac{\partial\chi'_1}{\partial x}\right) + \frac{1+a}{2}\frac{\partial\chi''_0}{\partial x}\frac{\partial\nabla^2_\perp\chi_0}{\partial x} + \frac{\partial\chi'_0}{\partial y}\frac{\partial^3\chi'_0}{\partial x^2\partial y} + \frac{\partial\chi'_0}{\partial x}\frac{\partial^3\chi'_0}{\partial x^3} \\ &\left.-\left(\nabla^2_\perp\chi_0\right)\frac{\partial^2\chi''_0}{\partial x^2}\right] - 2\frac{\partial^2\psi_1}{\partial x\partial y} - \frac{\partial^2\chi'_1}{\partial x^2} + \tau^{(1)}_{xx} \end{aligned} \tag{B.16}$$

$$
\begin{aligned}
0 =& 2FE\frac{\partial^2\chi_0'}{\partial x\partial y}\left(\nabla_\perp^2\chi_0+2a\nabla_\perp{}^2\chi_0'\right)\\
&-2FE\left(\frac{\partial\chi_0'}{\partial x}\frac{\partial^3\chi_0'}{\partial x^2\partial y}+\frac{\partial\chi_0'}{\partial y}\frac{\partial^3\chi_0'}{\partial x\partial y^2}\right)\\
&+FE(a+1)\left[\frac{\partial\chi_0''}{\partial x}\left(\frac{\partial\chi_1''}{\partial y}-\frac{\partial\psi_1'}{\partial x}\right)+\frac{\partial\chi_0''}{\partial y}\left(\frac{\partial\chi_1''}{\partial x}-\frac{\partial\psi_1'}{\partial y}\right)\right]\\
&+FEa\left(\frac{\partial\chi_0''}{\partial x}\frac{\partial\nabla_\perp^2\chi_0}{\partial y}+\frac{\partial\chi_0''}{\partial y}\frac{\partial\nabla_\perp^2\chi_0}{\partial x}\right)\\
&-\frac{(a+1)F}{2}\left(\tau_{yz}^{(1)}\frac{\partial\chi_0''}{\partial x}+\tau_{xz}^{(1)}\frac{\partial\chi_0''}{\partial y}\right)\\
&-\frac{(a+1)F}{2}\left[\tau_{yz}^{(0)}\left(\frac{\partial\chi_1''}{\partial x}+\frac{\partial\nabla_\perp^2\chi_0}{\partial x}+\frac{\partial\psi_1'}{\partial y}\right)+\tau_{xz}^{(0)}\left(\frac{\partial\chi_1''}{\partial y}+\frac{\partial\nabla_\perp^2\chi_0}{\partial y}-\frac{\partial\psi_1'}{\partial x}\right)\right]\\
&-F\left(a\tau_{xy}^{(0)}\nabla_\perp^2\chi_0'+\tau_{xy}^{(0)'}\nabla_\perp^2\chi_0\right)-2\frac{\partial^2\chi_1'}{\partial x\partial y}+\nabla_\perp^2\psi_1+\tau_{xy}^{(1)}\\
&+F\left[\frac{\partial\chi_0'}{\partial y}\frac{\partial\tau_{xy}^{(0)}}{\partial y}+\frac{\partial\chi_0'}{\partial x}\frac{\partial\tau_{xy}^{(0)}}{\partial x}\right]
\end{aligned}
\tag{B.17}
$$

$$
\begin{aligned}
0 =& FE\left[\left(\nabla_\perp^2\chi_0\right)\frac{\partial\chi_0''}{\partial x}-\frac{\partial\chi_0'}{\partial x}\frac{\partial^2\chi_0''}{\partial x^2}-\frac{\partial\chi_0'}{\partial y}\frac{\partial^2\chi_0''}{\partial x\partial y}\right]-F\tau_{xz}^{(0)'}\nabla_\perp^2\chi_0\\
&-2FE\frac{\partial\chi_0''}{\partial x}\left[\left(a+\frac{1}{2}\right)\frac{\partial^2\chi_0'}{\partial y^2}+\frac{\partial^2\chi_0'}{\partial x^2}\right]\\
&-\frac{F}{2}\frac{\partial\chi_0''}{\partial x}\left[(a-1)\tau_{xx}^{(0)}+\tau_{zz}^{(0)}\right]\\
&-2F\frac{\partial\chi_0''}{\partial y}\left[E\left(a-\frac{1}{2}\right)\frac{\partial^2\chi_0'}{\partial x\partial y}-\frac{a-1}{4}\tau_{xy}^{(0)}\right]\\
&-\frac{\partial\psi_1'}{\partial y}+F\frac{\partial\chi_0'}{\partial x}\frac{\partial\tau_{xz}^{(0)}}{\partial x}-Fa\left[\tau_{yz}^{(0)}\frac{\partial^2\chi_0}{\partial x\partial y}-\tau_{xz}^{(0)}\frac{\partial^2\chi_0'}{\partial y^2}\right]\\
&+\frac{\partial\nabla_\perp^2\chi_0}{\partial x}+F\frac{\partial\chi_0'}{\partial y}\frac{\partial\tau_{xz}^{(0)}}{\partial y}+\tau_{xz}^{(1)}-\frac{\partial\chi_1''}{\partial x}
\end{aligned}
\tag{B.18}
$$

$$
\begin{aligned}
0 =& 2FE\left[\left(\nabla_\perp^2\chi_0\right)\frac{\partial^2\chi_0''}{\partial y^2}-\frac{\partial\chi_0'}{\partial x}\frac{\partial^3\chi_0'}{\partial x\partial y^2}-\frac{\partial\chi_0'}{\partial y}\frac{\partial^3\chi_0'}{\partial y^3}\right]-2aF\tau_{xy}^{(0)}\frac{\partial^2\chi_0'}{\partial x\partial y}\\
&-2(a+1)F\frac{\partial\chi_0''}{\partial y}\left(\frac{\tau_{yz}^{(0)}}{2}+E\frac{\partial\psi_1'}{\partial x}\right)\\
&+2FE\frac{\partial\chi_0''}{\partial y}\left[(a+1)\frac{\partial\chi_1''}{\partial y}-a\frac{\partial\nabla_\perp^2\chi_0}{\partial y}\right]F\tau_{yz}^{(0)}\left[(a-1)\frac{\partial\nabla_\perp^2\chi_0}{\partial y}-(a+1)\frac{\partial\chi_1''}{\partial y}\right]\\
&+4aFE\left[\left(\frac{\partial^2\chi_0'}{\partial x\partial y}\right)^2+\left(\frac{\partial^2\chi_0'}{\partial y^2}\right)^2\right]-2aF\tau_{yy}^{(0)}\frac{\partial^2\chi_0'}{\partial y^2}-2\frac{\partial^2\chi_1'}{\partial y^2}\\
&+F(a+1)\tau_{yz}^{(0)}\frac{\partial\psi_1'}{\partial x}+2\frac{\partial^2\psi_1}{\partial x\partial y}-F\tau_{yy}^{(0)}\nabla_\perp^2\chi_0\\
&+\tau_{yy}^{(1)}+F\left(\frac{\partial\chi_0'}{\partial y}\frac{\partial\tau_{yy}^{(0)}}{\partial y}+\frac{\partial\chi_0'}{\partial x}\frac{\partial\tau_{yy}^{(0)}}{\partial x}\right)
\end{aligned}
\tag{B.19}
$$

$$
\begin{aligned}
0 =& FE\left[\left(\nabla_\perp^2\chi_0\right)\frac{\partial\chi_0'''}{\partial y}-\frac{\partial\chi_0'}{\partial x}\frac{\partial^2\chi_0''}{\partial x\partial y}-\frac{\partial\chi_0'}{\partial y}\frac{\partial^2\chi_0''}{\partial y^2}\right]+\frac{\partial\nabla_\perp^2\chi_0}{\partial y}\\
&-2FE\frac{\partial\chi_0''}{\partial y}\left[\left(a+\frac{1}{2}\right)\frac{\partial^2\chi_0'}{\partial x^2}+\frac{\partial^2\chi_0'}{\partial y^2}\right]\\
&-\frac{F}{2}\frac{\partial\chi_0''}{\partial y}\left[(a-1)\tau_{yy}^{(0)}+(a+1)\tau_{zz}^{(0)}\right]\\
&\times 2F\frac{\partial\chi_0''}{\partial x}\left[\left(a-\frac{1}{2}\right)E\frac{\partial^2\chi_0'}{\partial x\partial y}-\frac{(a-1)}{4}\tau_{xy}^{(0)}\right]\\
&+F\left(\frac{\partial\chi_0'}{\partial x}\frac{\partial\tau_{yz}^{(0)}}{\partial x}+\frac{\partial\chi_0'}{\partial y}\frac{\partial\tau_{yz}^{(0)}}{\partial y}\right)+Fa\tau_{yz}^{(0)}\frac{\partial^2\chi_0'}{\partial x^2}-Fa\tau_{xz}^{(0)}\frac{\partial^2\chi_0'}{\partial x\partial y}\\
&+\frac{\partial\psi_1'}{\partial x}-F\tau_{yz}^{(0)'}\nabla_\perp^2\chi_0-\frac{\partial\chi_1''}{\partial y}+\tau_{yz}^{(1)}
\end{aligned}
\tag{B.20}
$$

$$
\begin{aligned}
0 =& 2FE\left[\frac{\partial\chi_0'}{\partial x}\frac{\partial^3\chi_0'}{\partial x\partial y^2}+\frac{\partial\chi_0'}{\partial y}\frac{\partial^3\chi_0'}{\partial y^3}-\left(\nabla_\perp^2\chi_0''\right)\left(\nabla_\perp^2\chi_0\right)+2a\left(\frac{\partial^2\chi_0'}{\partial y^2}\right)^2\right]\\
&-F(a-1)\left[\tau_{xz}^{(0)}\frac{\partial^2\chi_1''}{\partial x^2}+\tau_{yz}^{(0)}\frac{\partial\chi_1''}{\partial y1}\right]\\
&+F(a+1)\left(\tau_{yz}^{(0)}\frac{\partial\nabla_\perp^2\chi_0}{\partial y}+\tau_{xz}^{(0)}\frac{\partial\nabla_\perp^2\chi_0}{\partial x}\right)\\
&+8Fa\frac{\partial^2\chi_0'}{\partial x^2}\left[E\frac{\partial^2\chi_0'}{\partial y^2}+\frac{\tau_{zz}^{(0)}}{4}\right]+F(1-a)\left[\tau_{xz}^{(0)}\frac{\partial\psi_1'}{\partial y}-\tau_{yz}^{(0)}\frac{\partial\psi_1'}{\partial x}\right]\\
&+4FEa\left(\frac{\partial^2\chi_0'}{\partial x^2}\right)^2-2FE\left(\frac{\partial\chi_0'}{\partial x}\frac{\partial^3\chi_0'}{\partial y^3}+\frac{\partial\chi_0'}{\partial y}\frac{\partial^3\chi_0'}{\partial x^2\partial y}\right)\\
&+2Fa\tau_{zz}^{(0)}\frac{\partial^2\chi_0'}{\partial y^2}+F\left(\frac{\partial\chi_0'}{\partial x}\frac{\partial\tau_{zz}^{(0)}}{\partial x}+\frac{\partial\chi_0'}{\partial y}\frac{\partial\tau_{zz}^{(0)}}{\partial y}\right)\\
&-2FE\frac{\partial\chi_0''}{\partial y}\left[(1-a)\frac{\partial\chi_1''}{\partial y}+a\frac{\partial\nabla_\perp^2\chi_0}{\partial y}\right]\\
&-2F(a-1)\frac{\partial\chi_0''}{\partial y}\left[\frac{\tau_{yz}^{(1)}}{2}+E\frac{\partial\psi_1'}{\partial x}\right]-2FE\frac{\partial\chi_0''}{\partial x}\left[(a-1)\frac{\partial\chi_1''}{\partial x}-a\frac{\partial\nabla_\perp^2\chi_0}{\partial x}\right]\\
&-2F(a-1)\frac{\partial\chi_0''}{\partial x}\left[\frac{\tau_{xz}^{(1)}}{2}-E\frac{\partial\psi_1'}{\partial y}\right]-F\tau_{zz}^{(0)'}\nabla_\perp^2\chi_0+\tau_{zz}^{(1)}+\nabla_\perp^2\chi_1'
\end{aligned}
\tag{B.21}
$$

At the order of approximation the corresponding boundary conditions are,

$$\frac{\partial\theta_1}{\partial z}=0 \quad \text{at} \quad z=0,1 \tag{B.22}$$

$$\frac{\partial\chi_1}{\partial z}=\chi_1=0 \quad \text{at} \quad z=0,1 \tag{B.23}$$

$$\psi_1=0 \quad \text{at} \quad z=0,1 \tag{B.24}$$

Finally, at $O(\epsilon^2)$ only the equation for temperature is needed. From this equation the second solvability condition is obtained. Thus,

$$
\begin{aligned}
\frac{\partial^2\theta_1}{\partial z^2}=&\frac{\partial\theta_0}{\partial\bar{t}}+\nabla_\perp^2\chi_1-\nabla_\perp^2\theta_1+\frac{\partial\chi_0'}{\partial y}\frac{\partial\theta_1}{\partial y}+\frac{\partial\chi_0'}{\partial x}\frac{\partial\theta_1}{\partial x}+\frac{\partial\psi_1}{\partial y}\frac{\partial\theta_0}{\partial x}\\
&-\frac{\partial\psi_1}{\partial x}\frac{\partial\theta_0}{\partial y}-\left(\nabla_\perp^2\chi_0\right)\frac{\partial\theta_1}{\partial z}
\end{aligned}
\tag{B.25}
$$

subjected to the following boundary conditions,

$$\frac{\partial \theta_2}{\partial z} = \overline{B}_L \theta_0 \quad \text{at} \quad z = 0 \tag{B.26}$$

$$\frac{\partial \theta_2}{\partial z} = -\overline{B}_U \theta_0 \quad \text{at} \quad z = 1 \tag{B.27}$$

## References


[1] H.M. Park, H.S. Lee, Nonlinear hydrodynamic stability of viscoelastic fluids heated from below, J. Non-Newtonian Fluid Mech. 60 (1995) 1–26.
[2] H.M. Park, H.S. Lee, Hopf bifurcations of viscoelastic fluids heated from below, J. Non-Newtonian Fluid Mech. 66 (1996) 1–34.
[3] J. Martínez–Mardones, R. Tiemann, D. Walgraef, W. Zeller, Amplitude equations and pattern selection in viscoelastic convection, Phys. Rev. E 54 (1996) 1478–1488.
[4] J. Martínez–Mardones, R. Tiemann, D. Walgraef, Convective and absolute instabilities in viscoelastic fluid convection, Physica A 268 (1999) 14–23.
[5] J. Martínez–Mardones, R. Tiemann, D. Walgraef, Rayleigh–Bénard convection in binary viscoelastic fluid, Physica A 283 (2000) 233–236.
[6] J. Martínez–Mardones, R. Tiemann, D. Walgraef, Thermal convection thresholds in viscoelastic solutions, J. Non-Newtonian Fluid Mech. 93 (2000) 1–15.
[7] J. Martínez–Mardones, R. Tiemann, D. Walgraef, Amplitude equation for stationary convection in a binary viscoelastic fluid, Physica A 327 (2003) 29–33.
[8] B. Albaalbaki, R.E. Khayat, Pattern selection in the thermal convection of non-Newtonian fluids, J. Fluid Mech. 668 (2011) 500–550.
[9] P. Kolodner, Oscillatory convection in viscoelastic DNA suspensions, J. Non-Newtonian Fluid Mech. 75 (1998) 167–192.
[10] D. Braun, N.L. Goddard, A. Libchaber, Exponential DNA replication by laminar convection, Phys. Rev. Lett. 91 (2003) 158103.
[11] D. Braun, PCR by thermal convection, Mod. Phys. Lett. B 18 (2004) 775–784.
[12] C.B. Mast, D. Braun, Thermal trap for DNA replication, Phys. Rev. Lett. 104 (2010) 188102.
[13] M.J. Beuchert, Y.Y. Podladchikov, Viscoelastic mantle convection and lithospheric stresses, Geophys. J. Int. 183 (2010) 35–63.
[14] L.A. Dávalos-Orozco, O. Manero, Thermoconvective instability of a second-order fluid, J. Phys. Soc. Jpn. 55 (1986) 442–445.
[15] L.A. Dávalos-Orozco, Viscoelastic natural convection, in: J. de Vicente (Ed.), Viscoelasticity – From Theory to Biological Applications, Intech, Rijeka, 2012, pp. 3–32.
[16] E.D. Siggia, A. Zippelius, Pattern selection in Rayleigh–Bénard convection near threshold, Phys. Rev. Lett. 47 (1981) 835–838.
[17] J.M. Massaguer, I. Mercader, Shear modes in low-Prandtl thermal convection, in: J.E. Wesfreid, S. Zaleski (Eds.), Cellular Structures in Instabilities, Springer-Verlag, Berlin, 1984, pp. 270–277.
[18] L.M. Pismen, Inertial effects in long-scale thermal convection, Phys. Lett. A 116 (1986) 241–244.
[19] E. Knobloch, Pattern selection in long-wavelength convection, Physica D 41 (1990) 450–479.
[20] L. Shtilman, G. Sivashinsky, Hexagonal structure of large-scale Marangoni convection, Physica D 52 (1991) 477–488.
[21] A.A. Golovin, A.A. Nepomnyashchy, L.M. Pismen, Pattern formation in large-scale Marangoni convection with deformable interface, Physica D 81 (1995) 117–147.
[22] A.A. Golovin, A.A. Nepomnyashchy, L.M. Pismen, Nonpotential effects in nonlinear dynamics of Marangoni convection, Int. J. Bifurcat. Chaos 12 (2002) 2487–2500.
[23] A. Oron, A.A. Nepomnyashchy, Long-wavelength thermocapillary instability with the Soret effect, Phys. Rev. E 69 (2004) 016313.
[24] M.R.E. Proctor, Planform selection by finite-amplitude thermal convection between poorly conducting slabs, J. Fluid Mech. 113 (1981) 469–485.
[25] S. Chapman, C.J. Childress, M.R.E. Proctor, Long wavelength thermal convection between non-conducting boundaries, Earth Planet. Sci. Lett. 51 (1980) 362–369.
[26] D.A. Nield, The onset of transient convective instability, J. Fluid Mech. 71 (1975) 441–454.
[27] M.W. Johnson, D. Segalman, A model for viscoelastic fluid behavior which allows non-affine deformation, J. Non-Newtonian Fluid Mech. 2 (1977) 255–270.
[28] I. Pérez-Reyes, L.A. Dávalos-Orozco, Effect of thermal conductivity and thickness of the walls in the convection of a viscoelastic Maxwell fluid layer, Int. J. Heat Mass Transfer 54 (2011) 5020–5029.
[29] P. Cerisier, S. Rahal, J. Cordonnier, G. Lebon, thermal influence of boundaries on the onset of Rayleigh–Bénard convection, Int. J. Heat Mass Transfer 41 (1998) 3309–3320.
[30] S.M. Cox, Long-wavelength thermal convection in a weak shear flow, IMA J. Appl. Math. 58 (1997) 159–184.
[31] S.M. Cox, The onset of thermal convection between poorly conducting horizontal boundaries in the presence of a shear flow, SIAM J. Appl. Math. 56 (1996) 1317–1328.
[32] E. Knobloch, J. De Luca, Amplitude equations for traveling wave convection, Nonlinearity 3 (1990) 975–980.
[33] A.C. Newell, J.A. Whitehead, Finite bandwidth, finite amplitude convection, J. Fluid Mech. 38 (1969) 279–303.
[34] L.A. Segel, Distant side-walls cause slow amplitude modulation of cellular convection, J. Fluid Mech. 38 (1969) 203–224.
[35] R. Hoyle, Pattern Formation: An Introduction to Methods, Cambridge University Press, Cambridge, 2006.
[36] P. Manneville, Instabilities, Chaos and Turbulence, Imperial College Press., London, 2004.
[37] R.B. Hoyle, Universal instabilities of rolls, squares and hexagons, in: P.A. Tyvand (Ed.), Time-dependent Nonlinear Convection, vol. 19, Computational Mechanics Publications, Southampton, 1998, pp. 83–114.
[38] S. Fauve, Pattern forming instabilities, in: C. Godréche, P. Manneville (Eds.), Hydrodynamics and Nonlinear Instabilities, Aléa-Saclay, Cambridge University Press, Cambridge, 1998, pp. 387–491.
[39] K. Fujimura, S. Yamada, Hexagons and triangles in the Rayleigh–Bénard problem: quintic-order equations on a hexagonal lattice, Proc. Roy. Soc. A 464 (2008) 2721–2739.